

Extraction of Lignin Using scCO₂ and Preparation of High-Performance Composite Films with Poly(vinyl alcohol)

Yan-Hong Feng,^{a,b,c,d} Fei-Ming Shi,^{a,b,c} Yun-Hao Zhang,^{a,b,c} Yue-Ping Jiang,^{a,b,c} Hang Sun,^{a,b,c} Bo Wu,^e and Xi-Ling Zhou^{a,b,c*}

Lignin (SCEL) was separated from steam-exploded eucalyptus wood fibers using a supercritical carbon dioxide (scCO₂)–ethanol/water composite medium, which was compared with traditional industrial alkaline extraction of lignin (AL) and high-temperature ethanol extraction of lignin (EL). All three kinds of lignin were spray-dried to form microparticles. The obtained SCEL, AL, and EL particles were mixed with poly(vinyl alcohol) (PVOH) to prepare a composite film. Compared with the pure PVOH film, the transmittance of the composite film to ultraviolet light was reduced from more than 70% to less than 20%, and the tensile strengths of the SCEL/PVOH, AL/PVOH, and EL/PVOH films were increased by 79.2%, 39.1%, and 66.0%, respectively. The water contact angle was increased from 35.5° to 95.3°, 59.5°, and 66.7°, respectively. In terms of performance improvement, SCEL had a better effect. The SCEL particle size was small and uniform, and SCEL contained more S-type structural units and β-O-4 bonds, which is conducive to its uniform dispersion in the PVOH matrix and increases the contact area between lignin and ultraviolet light, thereby improving its anti-ultraviolet performance. The hydrophilic groups in lignin form a large number of hydrogen bonds with PVOH, which promotes the combination of lignin and PVOH, and at the same time exposes a large number of hydrophobic groups of lignin, which improves the mechanical properties and the hydrophobicity of the film.

DOI: 10.15376/biores.17.4.6598-6616

Keywords: Supercritical carbon dioxide; Eucalyptus fiber; Lignin; PVOH; Composite film

Contact information: a: Guangdong Provincial Key Laboratory of Technique and Equipment for Macromolecular Advanced Manufacturing, South China University of Technology, Guangzhou 510641, PR China; b: Key Laboratory of Polymer Processing Engineering, Ministry of Education, South China University of Technology, Guangzhou 510641, PR China; c: National Engineering Research Center of Novel Equipment for Polymer Processing, South China University of Technology, Guangzhou 510641, PR China; d: The State Key Laboratory of Pulp and Paper, South China University of Technology, Guangzhou 510641, PR China; e: National Industrial Innovation Center of Polymer Materials Co., Ltd., Guangzhou, 510640, PR China; *Corresponding author: mexlzhou@scut.edu.cn

INTRODUCTION

There are many separation methods of lignin, and these can be divided into three types according to the principle: physical (Darus *et al.* 2020), chemical (Huang *et al.* 2020), and biological methods (Celiktas *et al.* 2019). Commonly used separation processes partially or completely destroy the structure of lignin, reducing its economic and utilization value. Therefore, an efficient and environmentally friendly lignin separation method is urgently needed. The goal is to achieve high-value utilization of lignin.

Supercritical carbon dioxide (scCO₂) is a fluid maintained above the critical temperature and the critical pressure, and it has properties of both gas and liquid. Because of its advantages of nontoxicity, low cost, wide source, low critical temperature, and chemical inertness (Lv *et al.* 2013), it has been used as a solvent for synthetic reactions and an extractant for natural product extraction (Stamenic *et al.* 2010). Because scCO₂ is a non-polar solvent, and lignin has a complex structure with both polar and nonpolar components, it is necessary to add a certain amount of polar components (entrainer) to pure scCO₂ to enhance its dissolution ability.

Lignin can be prepared as microparticles, which can be used in the fields of adsorbents (Li *et al.* 2016), antibacterial materials (Larrañeta *et al.* 2018), antioxidants (Lin *et al.* 2014), and composite materials (Yang *et al.* 2016). At present, the methods for preparing lignin particles include the antisolvent (Lievonon *et al.* 2016), self-assembly (Gao *et al.* 2019), chemical modification (Yiamsawas *et al.* 2014), and other methods. However, these methods require a variety of chemical reagents, and it is difficult to eliminate the impact of toxic reagents on the environment and in the subsequent applications. It is difficult to control the particle size using mechanical methods such as ultrasonic treatment (Agustin *et al.* 2019) or mechanical grinding (Nair *et al.* 2014). To prepare lignin particles with the ideal size, the spray drying method can reduce the use of organic solvents and control the size by adjusting the spray drying parameters.

The good biocompatibility and film-forming properties of PVOH give it broad application prospects in the field of environmental protection films. Lignin can form strong hydrogen bonds with PVOH, inhibit the process of thermal decomposition reaction, and improve the mechanical properties of the film. At the same time, because a large number of hydrophilic hydroxyl groups of PVOH form hydrogen bonds with lignin, the hydrophobicity of the film can be increased due to the exposure of the hydrophobic skeleton structure of lignin. In addition, the methoxy and aromatic ring structures of lignin also endow it with UV resistance. Yang *et al.* (2020) isolated lignin-containing nanofibers from wheat by acid solution combined with an ultrasonic method, and mixed with PVOH to prepare composites, which showed better waterproof, thermal, and mechanical properties. Ko *et al.* (2020) prepared an esterified PVOH–lignin resin that had good waterproof, thermal, mechanical, and adsorption properties. Although a large number of hydroxyl groups on the molecular chain of PVOH can improve its hydrogen-bonding ability with lignin, the content and type of functional groups of lignin itself caused by different extraction methods will affect its compatibility (Kadla and Kubo 2004). Therefore, it is necessary to explore a better extraction and separation method of lignin.

This study explored the extraction of lignin by scCO₂ combined medium and compared the structure and morphological properties of lignin extracted using the alkali and high-temperature ethanol methods. The effects on UV resistance, mechanical properties, and hydrophobicity of composite films were tested, and the extraction and preparation methods of lignin were optimized.

EXPERIMENTAL

Raw Materials

Five-year-old eucalyptus dry wood chips were procured from the fast-growing and high-yield forest base of Guangdong Dingfeng Paper Industry. The raw materials were pulverized and sieved with an 80-mesh screen. Polyvinyl alcohol (PVOH0588) was

obtained from the Sichuan Vinylon Plant of Sinopec Group.

The following reagents were used: absolute ethanol (analytical grade), NaOH (analytical grade), and HCl (38.5%), from Sinopharm Chemical Reagent Co., Ltd; deionized water, self-made, using a Guangzhou Congyuan Instruments Deionized Water Preparation Device; carbon dioxide (99.99%), from Guangzhou Shengtong Trading Co., Ltd; and deuterated dimethyl sulfoxide (DMSO-d₆) (99.8%), from Shanghai Aladdin Biochemical Technology Co., Ltd (Shanghai, China).

Extraction Methods of Lignin

scCO₂-ethanol/water lignin (SCEL)

Eucalyptus wood fiber and ethanol/water solution (ethanol/water = 1:1) were placed in a stainless-steel reactor (Haian Petroleum Scientific Research Instrument Co., Ltd, China) at a liquid–solid ratio of 20:1. The reactor was heated to 180 °C, the air was removed, and carbon dioxide was introduced until the pressure reached 12 MPa. After maintaining the pressure for 100 min, the temperature was reduced to 30 °C, and the extract was removed.

Alkali lignin (AL)

The eucalyptus fiber was fully immersed in a 5% NaOH aqueous solution, heated to 80 °C in a water bath, and stirred for 100 min. After the reaction, the reactant was filtered to obtain a filter residue and an extract.

Ethanol lignin (EL)

Eucalyptus wood fiber and ethanol/water solution (ethanol/water = 2:1) were placed in a stainless-steel reactor (Haian Petroleum Scientific Research Instrument Co., Ltd) at a liquid–solid ratio of 20:1. The reactor was heated to 180 °C, kept for 100 min, and then cooled to collect the extract.

Preparation of Lignin Microparticles

After cooling the extracts, they were diluted to the same concentration, and then spray-dried with a spray dryer (JOYN-8000T, Shanghai Jiuyue Electronic Technology Co., Ltd, Shanghai, China). The set temperature was 180 °C, and the feed rate was 500 mL/h. After drying, the spray-dried products of AL, EL, and SCEL were collected in a collection bottle at the bottom of the cyclone.

Preparation of Lignin/PVOH Composite Film

PVOH powder (2.5 g) was weighed and dissolved in 50 mL of deionized water and heated to 90 °C to fully dissolve it. Next, 3% lignin (calculated by the mass of PVOH) was added, and ultrasonically dispersed for 60 min to evenly mix it. The mixed solution was scraped evenly onto a clean glass plate at a temperature of 90 °C and then dried in a blast drying oven at 120 °C for 30 min. After the liquid was evaporated, the PVOH composite film was obtained.

Cellulose, Hemicellulose, and Lignin Content Test

Van Soest was used to determine the contents of cellulose, hemicellulose, and lignin in eucalyptus fiber raw materials and treated residues (Hindrichsen *et al.* 2006).

Chemical Structure Characterization

A Fourier transform infrared spectrometer (Nexus 670, ThermoNicolet, Waltham, MA, USA) was used to scan samples in the wavenumber range of 400 to 4000 cm^{-1} , and the number of scans was 32. The sample was KBr flakes containing 1% lignin and the composite film.

First, 50 mg of the completely dried lignin sample was dissolved in 0.6 mL of DMSO-d₆. The two-dimensional (2-D) HSQC NMR spectrum of the sample was collected using an NMR spectrometer (NEO 500M, Bruker, Karlsruhe, Germany) at 25 °C. The chemical shifts of the DMSO peaks ($\delta\text{C}/\delta\text{H}$ 39.5/2.5 ppm) were used for reference. Based on the semiquantitative characteristics of the 2-D nuclear magnetic correlation signal intensity, the relative proportions of different linkages can be calculated by integrating the relative signal intensities of the α positions of each linkage.

Scanning Electron Microscopy (SEM)

The lignin samples were observed using a field emission scanning electron microscope (FEI Quanta FEG 250, Hillsboro, OR, USA). A small amount of each dry specimen was fixed on the sample table with conductive adhesive. After gold spraying, the sample table was placed into the scanning electric mirror chamber, subjected to vacuum, and the samples were observed at an accelerating scanning voltage of 5 kV.

Thermal Stability

The thermal stability of the samples was analyzed using a thermogravimetric analyzer (TG, 209F3, Netzsch, Selb, Germany). The sample (5 to 10 mg) was placed in an alumina crucible, and the nitrogen flow rate was 50 mL/min. The test temperature range was 30 to 800 °C, and the heating rate was 10 °C/min.

Molecular Weight and its Distribution

Molecular weight and its distribution were determined for AL, EL, and SCEL by gel permeation chromatography (GPC) using an Agilent 1100 Series chromatograph (Agilent 1100, Agilent, Palo Alto, USA). To improve the solubility of the sample, the sample was acetylated and dissolved in tetrahydrofuran (THF) (Asikkala *et al.* 2012). Polystyrene standards of known molecular weight were used for reference. The test temperature was 23 °C, injection volume was 20 μL , and the flow rate was 1 mL/min.

UV Transmittance Test

The films were tested for UV transmittance using a UV-vis spectrophotometer (UV1900, Shimadzu, Kyoto, Japan) with a wavelength range of 190 to 800 nm.

Mechanical Property Test

The mechanical properties of the films were tested using an electronic universal material testing machine (ETM104B, Shenzhen Wantest Testing Equipment Co., Ltd, Shenzhen, China). The international standard ISO1184-1983 was used for tensile testing of plastic film. The film was cut into dumbbell-shaped sample strips with a total length of 75 mm, a gauge length of 20 mm, a narrow parallel part width of 4 mm, and an end width of 13 mm before the tensile properties were tested. A 1 kN sensor was used, and the tensile speed was set to 5 mm/min. Four replicates were done for each condition to calculate the average.

Water Contact Angle Test

The hydrophobicity of the PVOH/lignin composite films was tested using a surface tensiometer (DCAT21, DataPhysics, Stuttgart, Germany). The film was cut into a size of 2 cm × 2 cm, pasted on a glass slide, and placed on the stage of a static contact angle meter for contact angle testing. A drop of ultrapure water with a volume of 300 μL was dropped on the surface of the film, and then an appropriate baseline was selected to measure and record the contact angle.

RESULTS AND DISCUSSION

Cellulose, Hemicellulose, and Lignin Content

Compared with hemicellulose and lignin, cellulose is known to have the best chemical stability, so the change range of cellulose content is the smallest after the separation of different components. Therefore, the cellulose content in the raw materials was taken as the benchmark. It was assumed that the cellulose content remains unchanged after different lignin separation methods, the hemicellulose and lignin contents were obtained by Van Soest to obtain the data in Table 1.

Table 1. Composition Content of Eucalyptus Wood with Different Treatments (%) (Based on Cellulose Content)

Extraction Methods	Cellulose	Hemicellulose	Lignin	Lignin Extraction
Eucalyptus Raw Materials	48.94	13.88	24.79	0
scCO ₂ Treatment	48.94	3.59	6.21	74.9
Alkali Treatment	48.94	3.49	9.73	60.7
Ethanol Treatment	48.94	9.88	14.17	42.8

It can be seen from Table 1 that the raw cellulose content of eucalyptus fiber was 48.94%, hemicellulose content was 13.88%, and lignin content was 24.79%. After the three treatments, lignin could be removed to varying degrees. The removal efficiency of supercritical fluid method was the highest, because the supercritical fluid has good permeability and can fully penetrate the plant fiber skeleton. Compared with the alkali method, the supercritical fluid has higher solubility for lignin and can dissolve more lignin. At the same time, compared with the ethanol method, the supercritical fluid method will form carbonic acid in the extraction process, which is formed due to the interaction of carbon dioxide and water. The glycosidic bond in lignin has low acid stability, so it is easier to be destroyed under supercritical fluid treatment. More degraded lignin molecules diffuse from the surface of plant fibers to the solution, and they finally dissolve with assistance of the ethanol cosolvent.

Chemical Structure

Figure 1 shows the infrared spectrum of eucalyptus lignin extracted using different methods, wherein 2931 to 2933 cm⁻¹ is the absorption peak of saturated methylene stretching vibrations, 1383 cm⁻¹ is the absorption of the O–H stretching vibration in a phenolic hydroxyl group, 1329 cm⁻¹ is the syringyl aromatic ring, 1270 cm⁻¹ is the absorption peak of the lignin methoxy group, and 1122 cm⁻¹ is the C–O stretching vibration of the lignin S unit. Comparing the infrared spectra of SCEL and AL, the peaks in AL are

weaker than those in SCEL, indicating that NaOH reacted with the active phenolic hydroxyl and methoxy groups on the lignin S unit, destroying this structural unit (Alves-Ferreira *et al.* 2021), and the supercritical fluid can keep the structure of the S unit from being destroyed as much as possible because of its chemical inertness.

The peak at 1730 cm^{-1} is the C=O stretching vibration of the acetyl group and uronic acid group of polyxylose, and 1223 cm^{-1} is the C–O stretching vibration of the acetyl group. The two characteristic peaks of hemicellulose in EL had relatively high intensities, which shows that the high-temperature ethanol method has difficulty destroying the bonds between lignin and hemicellulose, whereas the intensity of these two characteristic peaks in SCEL weakens or even disappears. This result shows that the supercritical fluid can destroy the bonds of lignin–carbohydrate complexes and improve the purity of lignin products.

The stretching vibration peaks of the lignin benzene ring skeleton are at 1380 to 1600 cm^{-1} . SCEL, AL, and EL showed the same characteristic peaks in this range, which proved that the structure of the benzene ring was preserved. Therefore, from the perspective of the change of functional groups, the degradation mainly occurred in the groups and connecting bonds of the side chain (Li *et al.* 2019).

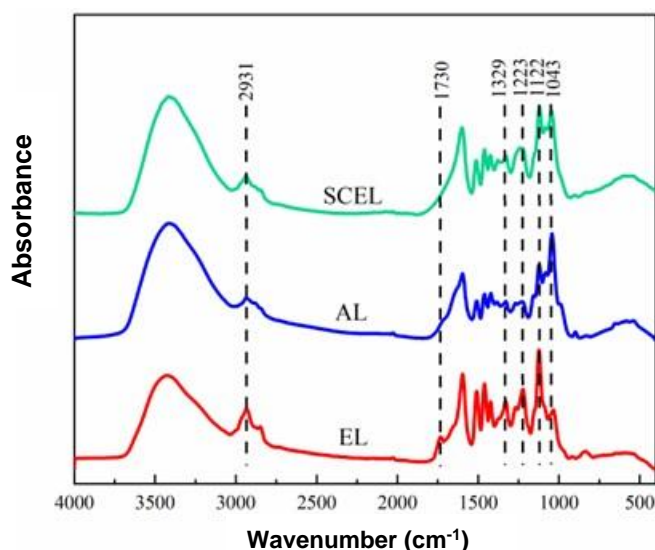


Fig. 1. Infrared spectra of eucalyptus lignin extracted using different treatment methods

Figure 2 shows the 2-D HSQC NMR spectra of lignin obtained using the three treatments and the main structural units of lignin. The structures are shown in Fig. 3. In the aromatic region, three basic structural units of lignin can be seen, and in the side chain region, there were different linkages such as β -O-4, β - β' , and β -5. G-type lignin was found in the aromatic region $\delta\text{C}/\delta\text{H}$ 115.70/6.74 ppm (Fig. 2G). The characteristic chemical shifts of the benzene rings of S-type lignin (Fig. 3 S, S') were found at $\delta\text{C}/\delta\text{H}$ 104.02/6.64 ppm and $\delta\text{C}/\delta\text{H}$ 107.30/7.21 ppm, indicating that eucalyptus lignin is a typical S/G-type lignin. Among them, the S/G value of SCEL was 2.76, the S/G value of AL was 1.40, and the S/G value of EL was 2.17. This is due to the relatively weak stability of the S-type structural unit. The phenolic hydroxyl group attached to the ring can react with NaOH to form a sodium salt, and OH^- is a nucleophile that can make the methoxy group undergo a nucleophilic substitution reaction to generate methanol.

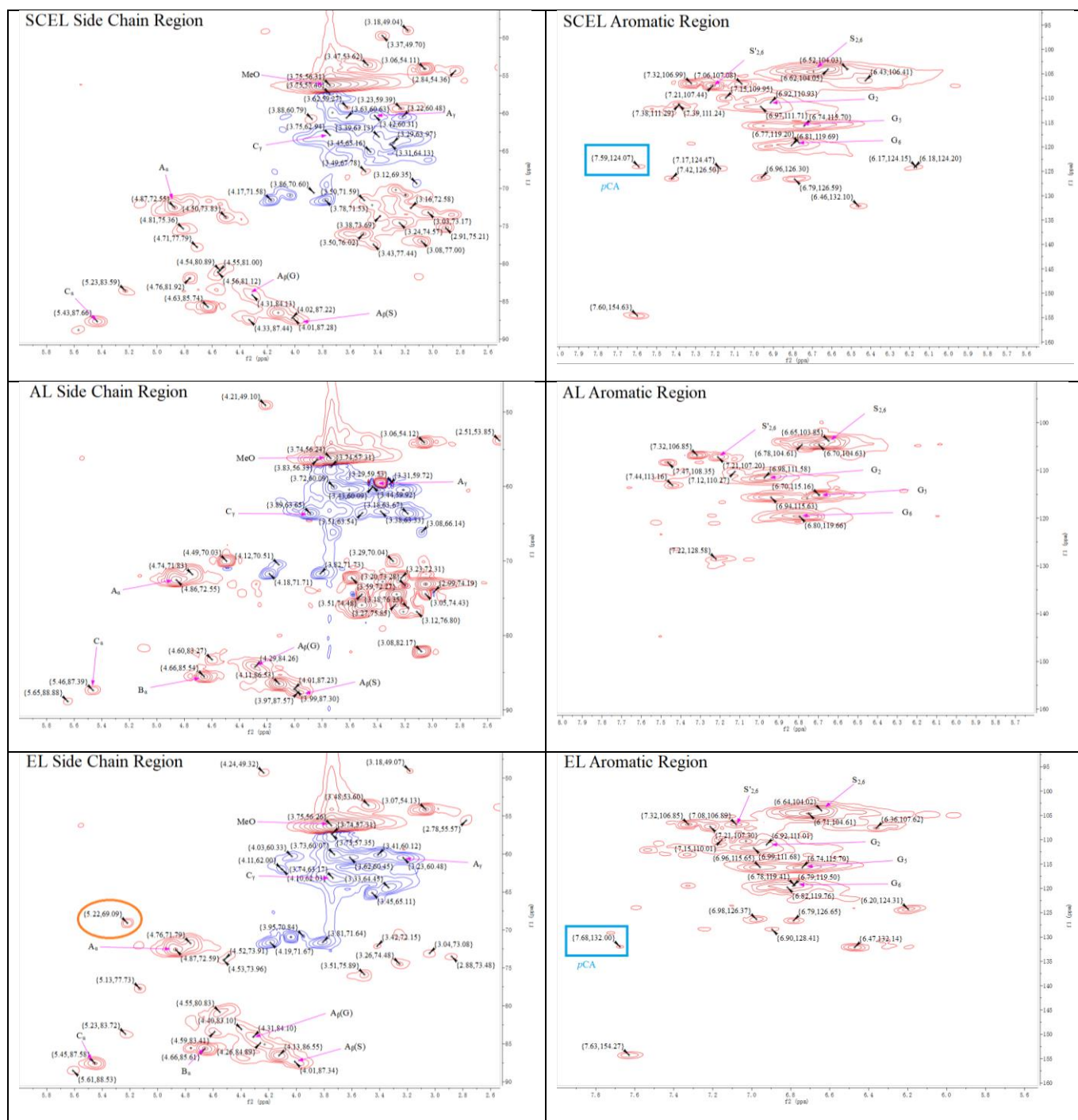


Fig. 2. 2-D NMR spectra of SCEL, AL and EL

The polarity of the S-type structural unit is weak (Jiang *et al.* 2020), so it is easier for the nonpolar scCO₂ combined with entrainers to dissolve the S-type structural unit; therefore the lignin treated with supercritical fluid contains more S-type structural units, and the large number of methoxy groups contained in the S unit also makes SCEL more hydrophobic.

The main connecting bonds between lignin building blocks are ether bonds and carbon-carbon bonds, as shown in Fig. 2. The content of β -O-4 bonds in SCEL was 66.07%, the content of β -O-4 bonds in AL was 28.03%, and the content of β -O-4 bonds in

EL was 44.06%. The high ether bond content provides more hydrogen bond acceptors, making it easier for SCEL to form hydrogen bonds with PVOH, which contains hydrogen bond donors. The hydroxyl groups in lignin can form ether bonds or double bonds through reversible etherification and carbonylation reactions in an ethanol solution, and the presence of $scCO_2$ can reduce the overall activation energy of the system, making the reaction more likely to occur, thereby forming more β -O-4 bonds (Zhang and Wu 2015).

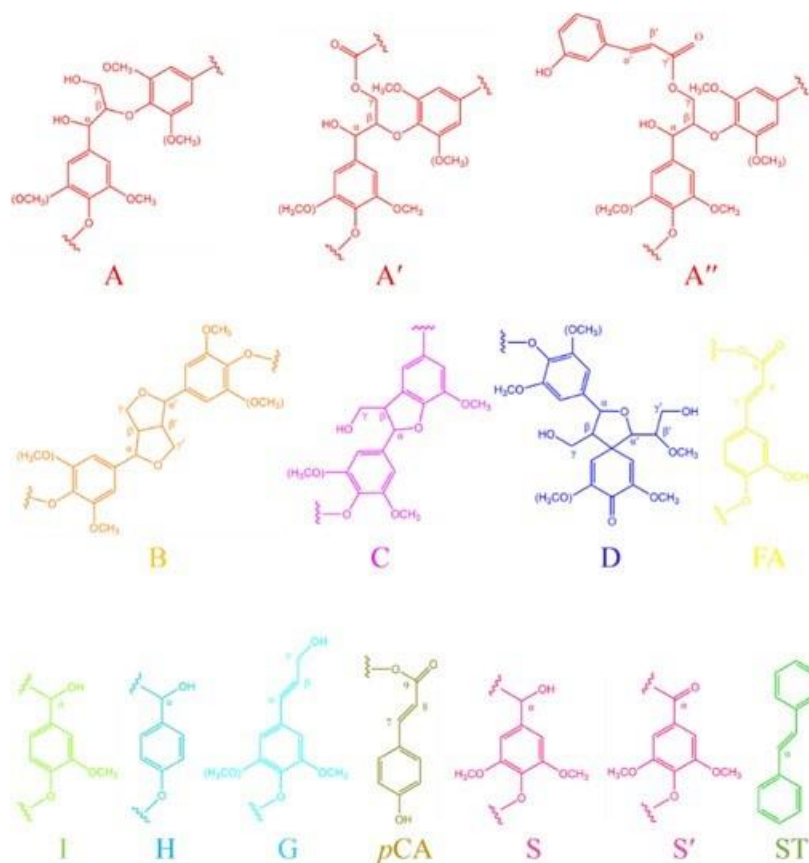


Fig. 3. Main structural units of lignin

The least content of β -O-4 in AL may be due to the easy destruction of ether bonds by the action of strong bases. Similarly, in the side chain region, a clear signal for *p*-coumaryl ester (At the blue box in Figure 2) appeared at $\delta C/\delta H$ 124.07/7.59 ppm for SCEL and $\delta C/\delta H$ 132.00/7.68 ppm for EL (Zhang *et al.* 2018), whereas this was not found in AL. The characteristic signal of the structure indicated that NaOH reacted with the phenolic hydroxyl group and methoxy group on the benzene ring to deprotonate the phenolic hydroxyl group of the lignin, resulting in the decrease of its content (Wang *et al.* 2017).

In EL, methylene C–H in the ester bond between lignin and glucoside appeared at $\delta C/\delta H$ 69.09/5.22 ppm (at the orange box in Fig. 2), and the benzylic ether bond of lignin and carbohydrate (BE) appeared at $\delta C/\delta H$ 80.83/4.55 ppm, whereas there were no such characteristic signals in SCEL and AL, which further demonstrates that both the acidic environment provided by supercritical fluid treatment and the alkaline environment provided by alkali treatment can effectively destroy the bond between lignin and carbohydrates, reduce the content of hemicellulose in the extract, and improve the extracted lignin product purity.

Micromorphology

Figures 4a and 4b show that the AL product had a larger size and an average particle size of more than 100 μm . This is because the alkaline environment hinders the self-assembly of lignin, which makes it difficult to form particles with regular morphology. Because the alkaline lignin extract is a colloidal suspension, under the interaction between the hydrophilic groups and the hydrophobic group, the amorphous lignin molecules are more likely to agglomerate and combine to form an irregular network structure, which made it difficult to form small particles during spray drying.

Figures 4c and 4d show that although there were independent lignin particles in the EL, there were many flocculent structures on the surface of the particles, and the particles were bonded together, making the size larger. The average particle size was about 10 μm . The presence of flocculent material further shows that there were more hemicellulose impurities in EL.

In Figs. 4e and 4f, the particles of SCEL had an independent spherical uniform distribution, with an average particle size of 800 nm, and the surface of the particles was smooth and free of impurities, which shows that the hemicellulose in SCEL extract was significantly lower than that in EL extract. The hydrophilic group of lignin interacts with water during the dissolution process and the hydrophobic backbone interacts with ethanol, and these interactions drive the self-assembly of lignin to form spherically shaped microparticles, so higher purity lignin will show better microparticle preparation.

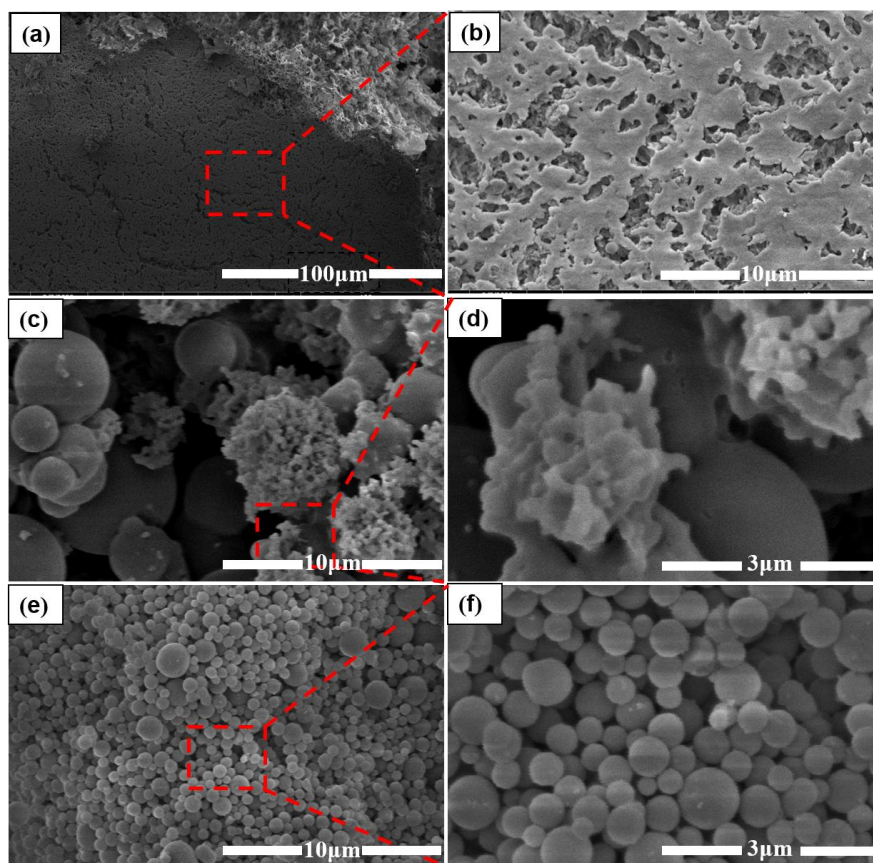


Fig. 4. Scanning electron microscopy (SEM) images of eucalyptus lignin extracted using different treatment methods: (a), (b) AL; (c), (d) EL; (e), (f) SCEL

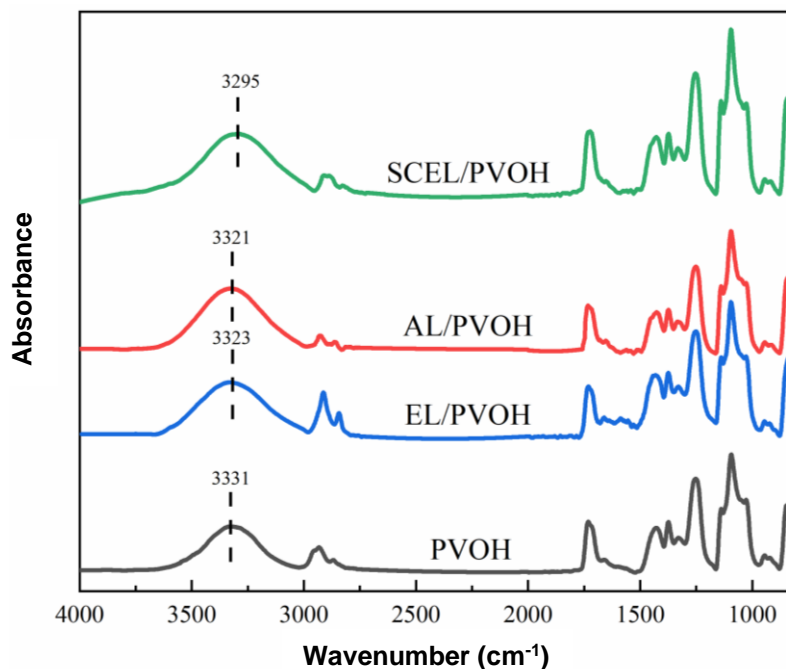


Fig. 5. Infrared spectrum of the composite films

Infrared Spectroscopy of Thin Films

The infrared spectrum of the lignin/PVOH composite film is shown in Fig. 5. It is difficult to find the characteristic peaks of lignin in the spectrum because the content of lignin in the composite system was only 3%, which is very small. The content is such that the characteristic peaks of lignin were masked by the characteristic peaks of PVOH. The range of 3000 to 3500 cm^{-1} in the infrared spectrum is the stretching vibration absorption of hydroxyl groups. After adding lignin, the peak position shifted to lower wavenumbers, which is attributed to the formation of strong hydrogen bonds in the film. Infrared spectroscopy showed that there was no chemical reaction during the blending modification of lignin and PVOH, only the formation of hydrogen bonds. The SCEL can expose more hydroxyl groups and β -O-4 bonds to form intermolecular hydrogen bonds with PVOH because of good particle dispersion.

Lignin and Film Thermal Stability

Figure 6 shows the TG–DTG curves of different kinds of lignin. The initial decomposition temperature of AL was the lowest, and the maximum thermal decomposition temperature was around 333.3 °C. Table 2 shows that the polydispersity index (PDI) of AL was relatively large, which indicates that there were both small molecular inorganic substance and macromolecular lignin in AL. This was because the action of strong alkali destroyed a large number of lignin bonds to form low molecular weight lignin, which decomposed at a lower temperature, so the DTG curve of AL appeared bimodal. At the same time, the condensation reaction occurred during the alkali treatment of AL, the degraded small-molecule phenols repolymerized to form condensed lignin containing more C–C bonds and the energy required to break the C–C bonds was much higher than that of the ether bonds. Therefore, the carbon residue extent of AL was significantly improved compared with the other two, reaching 41.85%, as shown in Table 3.

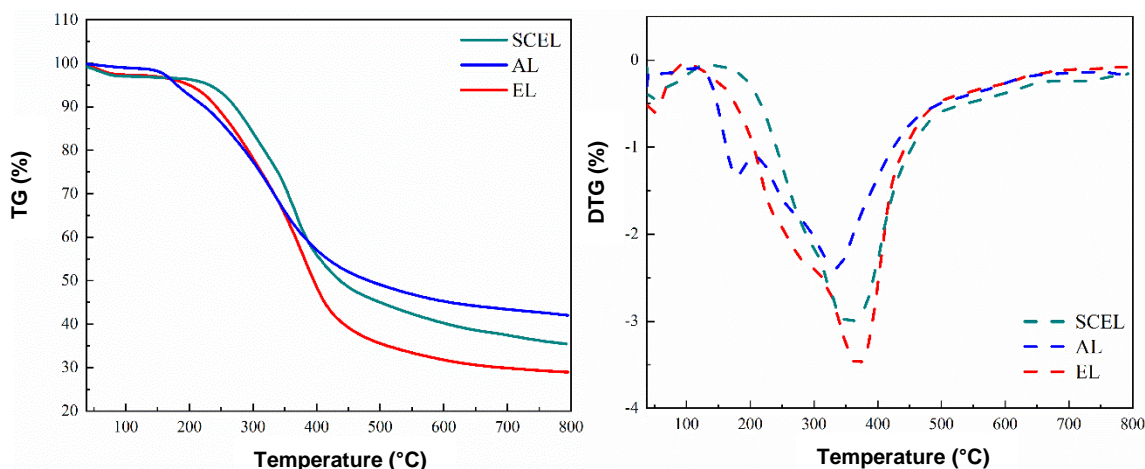


Fig. 6. TG–DTG curves of lignin extracted using different treatment methods.

Table 2. Number Average Molecular Weight (M_n), Weight Average Molecular Weight (M_w), and Polydispersity Index (PDI) of Lignin

Types of Lignin	M_n (g/mol)	M_w (g/mol)	PDI
SCEL	2296	4023	1.75
AL	2039	4740	2.32
EL	1587	2693	1.70

EL had a thermal decomposition shoulder peak at 250 to 300 °C because it was difficult to remove hemicellulose effectively using the high-temperature ethanol method, and it would dissolve together with lignin in the form of a lignin–carbohydrate complex, so at 250 to 300 °C the thermal decomposition peak of hemicellulose appeared.

Table 3. Carbon Residual Extent and Main Thermal Decomposition Temperature of Lignin

Types of Lignin	Residual Carbon (%)	Initial Thermal Decomposition Temperature (°C)	Termination Thermal Decomposition Temperature (°C)	Maximum Thermal Decomposition Rate Temperature (°C)
SCEL	35.43	261.7	666.9	360.1
AL	41.85	198.3	688.3	333.3
EL	28.91	236.4	673.7	368.7

The obvious weakening of the shoulder peak of hemicellulose in SCEL is due to the acidic environment during SCEL extraction. Because of the influence of carbonic acid, a large amount of acidic hydrolysis of hemicellulose occurs and the connection between lignin and hemicellulose is destroyed, so the obtained lignin is purer.

Figure 7 shows that 200 to 400 °C was the main decomposition range of PVOH. Compared with pure PVOH, the addition of lignin increased the maximum decomposition temperature of the films from 312 °C (PVOH film) to 314 °C (AL/PVOH film), 320 °C (EL/PVOH film), and 328 °C (SCEL/PVOH film), and the peak height of the DTG decreased, which indicates that the degradation rate of the film becomes slower after adding lignin (Zhang *et al.* 2019). This is because the removal of hydroxyl groups occurs during the thermal decomposition of PVOH, so the stability of the hydroxyl groups will

determine the stability of the film. After the addition of lignin, the strong interaction between lignin and the hydroxyl groups of PVOH to form intermolecular hydrogen bonds greatly restricted the movement of the PVOH segments (Zhang *et al.* 2020), which made the removal of hydroxyl groups require more energy. At the same time, the aromatic structure of lignin can form a structure similar to hindered phenols, which can capture the free radicals formed during the decomposition of PVOH in the process of thermal decomposition, thereby inhibiting the reaction process of thermal decomposition. Aromatic structural units also play an important role in improving thermal stability (Luo *et al.* 2021). SCEL can form more hindered phenolic structures because of the dissolution of more S-type lignin, which reduces the degradation extent of the film the most and increases the maximum decomposition temperature the most.

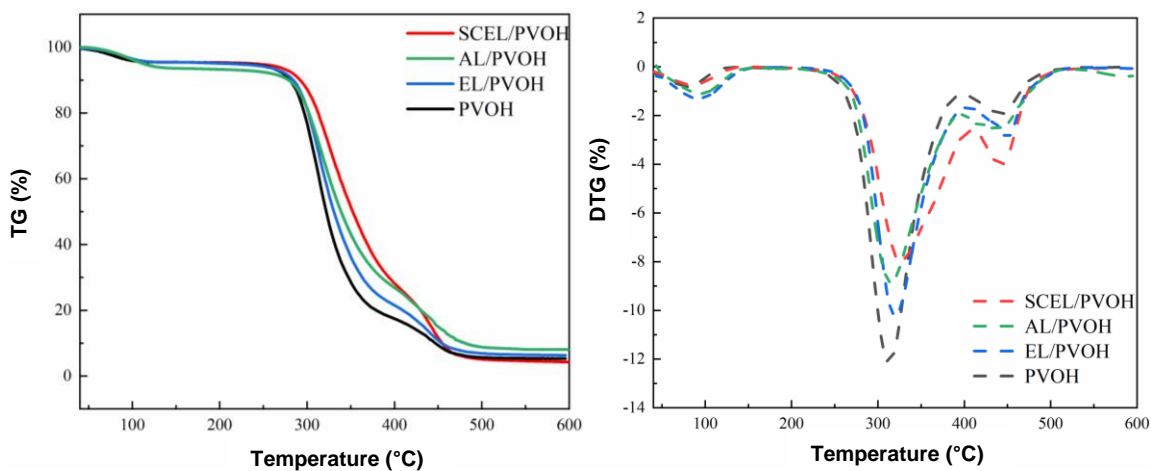


Fig. 7. TG–DTG curves of composite films

Film UV Resistance

Pure PVOH film has almost no blocking ability to light in the ultraviolet wavelength range, and it is colorless and transparent. As shown in Fig. 8, when lignin was added, the film appeared brown and the transmittance of ultraviolet light was significantly decreased.

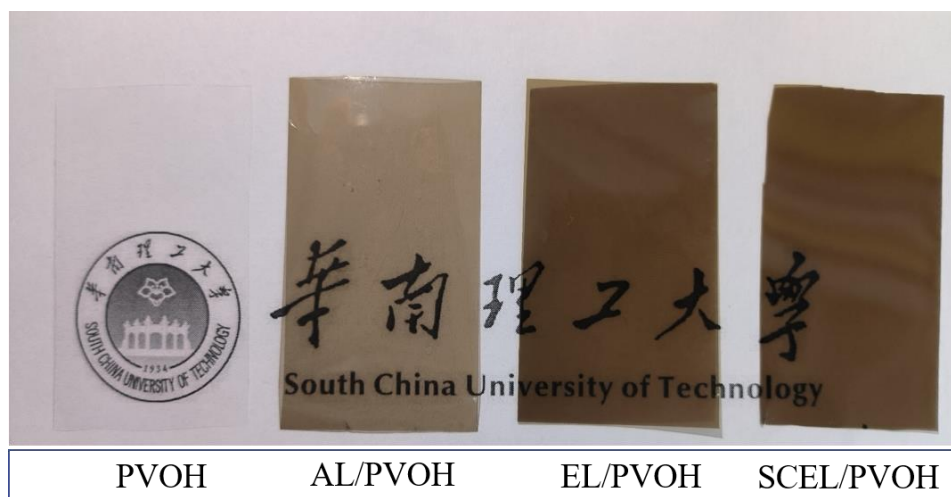


Fig. 8. Color contrast of composite films

The dark coloration is because the structure of lignin has more aromatic rings and conjugated double bonds (Monteiro *et al.* 2021), such as phenols, ketones, methoxy and other chromophoric groups. The conjugated system formed between these groups improves lignin's anti-ultraviolet properties (Huang *et al.* 2021). The color of AL/PVOH was the lightest. This is because alkali treatment destroys a large number of lignin color rendering groups, so its UV resistance is also the weakest. EL/PVOH and SCEL/PVOH exhibited similar colors, but SCEL/PVOH has better UV resistance because SCEL contains more methoxy groups. As an important electron donor group, methoxy groups can form larger conjugated systems with other components, which play an important role in the performance of UV resistance.

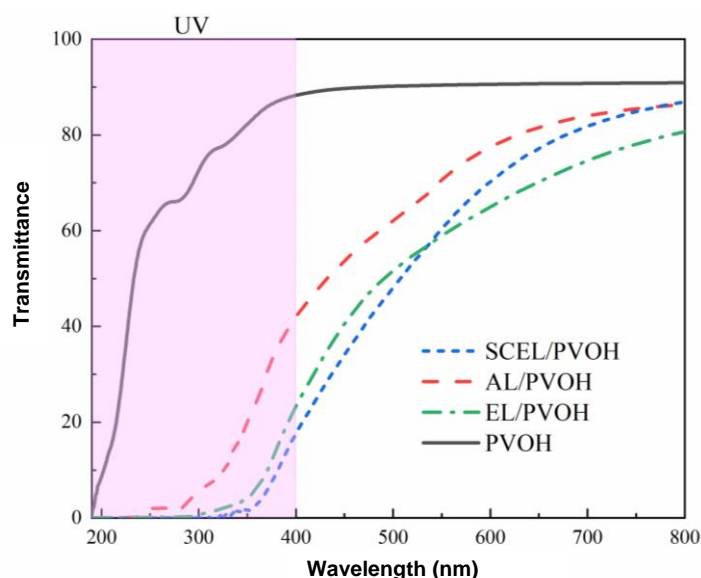


Fig. 9. UV resistance of PVOH and PVOH composite films

The addition of smaller size lignin particles also resulted in films with higher UV blocking efficiency. Under the same addition amount, the UV transmittance of the film with added SCEL was the lowest because, compared with AL and EL, SCEL has a larger surface area and can be more uniformly dispersed in the film system, so when the ultraviolet rays are irradiated on the film, there is more contact area with the lignin, which promotes the absorption of ultraviolet rays.

Film Mechanical Properties

Figure 10 shows the mechanical properties of the composite film. The tensile strength of pure PVOH was lower and the elongation at break was higher because the flexibility of the PVOH molecular chain was higher, and the relaxation process of the molecular chain is fast, so it had better ductility in the stretching process. The tensile strength of the three films prepared after adding lignin increased, but the elongation at break decreased. This is because both PVOH and lignin contain a large number of hydroxyl groups, and the intermolecular hydrogen bonds formed by the two enhance the compatibility between the matrix and the filler. Thus, the PVOH is closely combined with the rigid lignin particles, and the rigid particles can better withstand the stress load, causing the crack propagation path to change, thereby improving the tensile strength of the composite material and reducing the elongation at break (Posoknistakul *et al.* 2020).

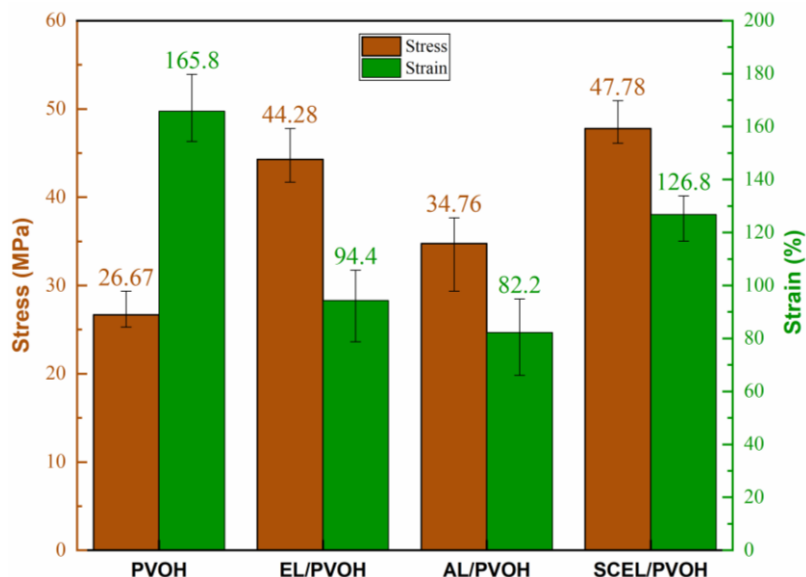


Fig. 10. Tensile strength and elongation at break of composite films

SCEL can form small-sized spherical particles during the particle preparation process, whereas AL had the function of a cross-linking bridge because of the presence of etherified phenolic acid groups, making it difficult to form independent particles during drying (Jacquet *et al.* 1995), and EL was easily agglomerated to form large particles because of the influence of impurities such as hemicellulose. Therefore, because of the small particle size and large specific surface area of SCEL, a large number of strong hydrogen bonds can be formed with PVOH, forming a network entanglement structure, which significantly enhances the tensile strength of SCEL/PVOH. In addition, SCEL has more β -O-4 bonds than AL and EL, which can form more hydrogen bonds with PVOH, which further promotes the improvement of the mechanical properties of SCEL/PVOH films.

Film Water Contact Angle

The water contact angle of pure PVOH film is only 35.5° , which is because the side chain of the PVOH molecular chain contains a large number of hydroxyl groups, which can form hydrogen bonds with water, making it extremely hydrophilic (Zhao *et al.* 2018). Because lignin is an amphiphilic compound with a hydrophobic phenylpropane skeleton structure and hydrophilic hydroxyl functional groups, when it is blended with PVOH to prepare films, a large number of hydroxyl groups in the PVOH structure form hydrogen bonds with the hydrophilic groups of lignin, reducing the binding effect with water. Moreover, a structure with hydrophilic groups facing inward and a hydrophobic skeleton facing outward is formed, which helps to hinder the penetration of water molecules into the film (Ni *et al.* 2022), so the addition of lignin enhanced the hydrophobicity of the film.

The SCEL-added film had the largest water contact angle. It is presumed that the particles of SCEL had the characteristics of small size, large specific surface area and high content of β -O-4 bonds. These can be more uniformly distributed in the PVOH matrix during the film preparation process, thus promoting the formation of hydrogen bonds between lignin and PVOH. When the polar hydroxyl groups on PVOH form hydrogen bonds with polar groups such as hydroxyl groups and ether bonds on lignin, the nonpolar groups on lignin are fully exposed, especially the S-type structural unit. The polarity of S-

type lignin is lower than that of G-type lignin, whereas the S/G value of SCEL is as high as 2.76, thus, SCEL/PVOH film showed better hydrophobicity.

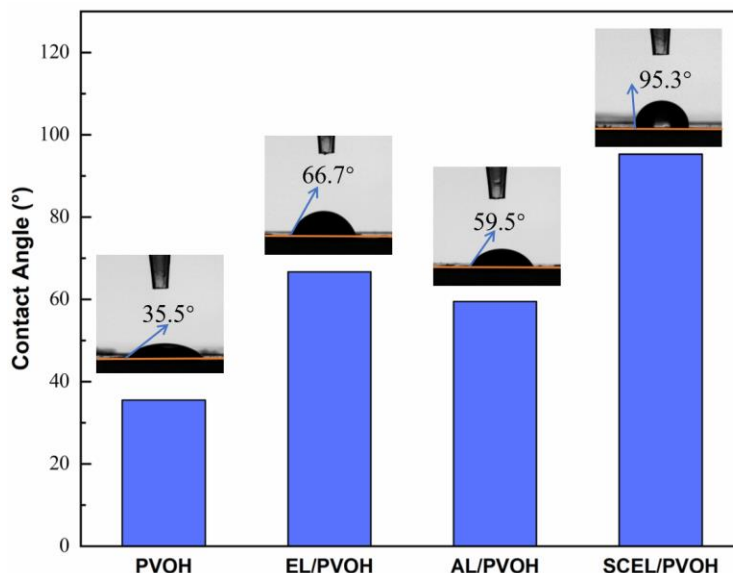


Fig. 11. Water contact angle of composite films

CONCLUSIONS

1. Lignin was extracted from eucalyptus fiber using the supercritical carbon dioxide (scCO₂)-ethanol/water medium, high-temperature ethanol, and alkali methods. Because of the supercritical fluid's strong permeability and diffusivity, under high-temperature and high-pressure conditions and the weakly acidic environment provided by CO₂ and water, it can penetrate the interior of the cell wall and destroy the bonds between lignin and carbohydrates. The scCO₂ separation method could not only separate the lignin with high efficiency but also the obtained lignin product had a higher content of S-type structural units than the alkaline method and higher purity than that of the high-temperature ethanol method. This means that the supercritical fluid extraction process can obtain lignin with high content of active groups and high purity.
2. Based on the advantages of high purity of steam-exploded eucalyptus lignin (SCEL) and high content of S-type structural units, when using the spray drying method to prepare lignin particles, SCEL had the characteristics of a smooth surface, with a smaller and more uniform particle size than AL and EL.
3. After blending these three kinds of lignin with poly(vinyl alcohol) (PVOH), the thermal stability, UV resistance, mechanical properties, and water resistance of the three composite films were improved compared with those of the pure PVOH film, and the composite film with SCEL had the best performance. SCEL with high S-type structural unit and β -O-4 bond content, high purity, and small and uniform particle size distribution can give the composite film the best performance when mixed with PVOH.

ACKNOWLEDGEMENTS

This work was supported by the National Natural Science Foundation of China (No. 51873073, 52273088), Natural Science Foundation of Guangdong Province (No. 2022A1515011561).

Declaration of Competing Interest

The authors declare that they have no competing interests.

Supporting Information

Supporting information may be found in the online version of this article.

REFERENCES CITED

- Agustin, M. B., Penttilä, P. A., Lahtinen, M., and Mikkonen, K. S. (2019). "Rapid and direct preparation of lignin nanoparticles from alkaline pulping liquor by mild ultrasonication," *ACS Sustainable Chemistry & Engineering* 7(24), 19925-19934. DOI: 10.1021/acssuschemeng.9b05445
- Alves-Ferreira, J., Lourenço, A., Morgado, F., Duarte, L. C., Roseiro, L. B., Fernandes, M. C., Pereira, H., and Carvalheiro, F. (2021). "Delignification of *Cistus ladanifer* biomass by organosolv and alkali processes," *Energies* 14(4), article no. 1127. DOI: 10.3390/en14041127
- Asikkala, J., Tamminen, T., and Argyropoulos, D. S. (2012). "Accurate and reproducible determination of lignin molar mass by acetobromination," *Journal of Agricultural and Food Chemistry* 60(36), 8968-8973. DOI: 10.1021/jf303003d
- Celiktas, M. S., Yaglikci, M., and Maleki, F. K. (2019). "Subcritical water extraction derived lignin for creation of sustainable reinforced composite materials," *Polymer Testing* 77, article no. 105918. DOI: 10.1016/j.polymertesting.2019.105918
- Darus, S. A. A. Z. M., Ghazali, M. J., Azhari, C. H., Zulkifli, R., Shamsuri, A. A., Sarac, H., and Mustafa, M. T. (2020). "Physicochemical and thermal properties of lignocellulosic fiber from *Gigantochloa scortechinii* bamboo: Effect of steam explosion treatment," *Fibers Polym.* 21, 2186-2194. DOI: 10.1007/s12221-020-1022-2
- Gao, Weijue, and Pedram Fatehi. (2019). "Lignin for polymer and nanoparticle production: Current status and challenges," *The Canadian Journal of Chemical Engineering* 97(11), 2827-2842. DOI: 10.1002/cjce.23620
- Hindrichsen, I. K., Kreuzer, M., Madsen, J., and Knudsen, K. B. (2006). "Fiber and lignin analysis in concentrate, forage, and feces: Detergent versus enzymatic-chemical method," *Journal of Dairy Science* 89(6), 2168-2176. DOI: 10.3168/jds.s0022-0302(06)72287-1
- Huang, D.-L., Li, R.-J., Xu, P., Li, T., Deng, R., Chen, S., and Zhang, Q. (2020). "The cornerstone of realizing lignin value-addition: Exploiting the native structure and properties of lignin by extraction methods," *Chemical Engineering Journal* 402, article no. 126237. DOI: 10.1016/j.cej.2020.126237
- Huang, J.-B., Guo, Q., Zhu, R.-N., Liu, Y.-Y., Xu, F., and Zhang, X.-M. (2021). "Facile fabrication of transparent lignin sphere/PVOH nanocomposite films with excellent UV-shielding and high strength performance," *International Journal of Biological*

- Macromolecules* 189, 635-640. DOI: 10.1016/j.ijbiomac.2021.08.167
- Jacquet, G., Pollet, B., Lapiere, C., Mhamdi, F., and Rolando, C. (1995). "New ether-linked ferulic acid-coniferyl alcohol dimers identified in grass straws," *Journal of Agricultural and Food Chemistry* 43(10), 2746-2751. DOI: 10.1021/jf00058a037
- Jiang, Y.-P., Feng, Y.-H., Lei, B., and Zhong, H.-T. (2020). "Impact mechanisms of supercritical CO₂-ethanol-water on extraction behavior and chemical structure of eucalyptus lignin," *International Journal of Biological Macromolecules* 161, 1506-1515. DOI: 10.1016/j.ijbiomac.2020.07.318
- Kadla, J. F., and Kubo, S. (2004). "Lignin-based polymer blends: Analysis of intermolecular interactions in lignin-synthetic polymer blends," *Composites Part A: Applied Science and Manufacturing* 35(3), 395-400. DOI: 10.1016/j.compositesa.2003.09.019
- Ko, H.-U., Kim, J. W., Kim, H. C., Zhai, L.-D., and Kim, J.-H. (2020). "Esterified PVOH-lignin resin by maleic acid applicable for natural fiber reinforced composites," *Journal of Applied Polymer Science* 137(26), article no. 48836. DOI: 10.1002/app.48836
- Larrañeta, E., Imizcoz, M., Toh, J. X., Irwin, N. J., Ripolin, A., Perminova, A., Dominguez-Robles, J., Rodriguez, A., and Donnelly, R. F. (2018). "Synthesis and characterization of lignin hydrogels for potential applications as drug eluting antimicrobial coatings for medical materials," *ACS Sustainable Chemistry & Engineering* 6(7), 9037-9046. DOI: 10.1021/acssuschemeng.8b01371
- Lin, X.-L., Zhou, M.-S., Wang, S.-Y., Lou, H.-M., Yang, D.-J., and Qiu, X.-Q. (2014). "Synthesis, structure, and dispersion property of a novel lignin-based polyoxyethylene ether from kraft lignin and poly (ethylene glycol)," *ACS Sustainable Chemistry & Engineering* 2(7), 1902-1909. DOI: 10.1021/sc500241g
- Li, J.-B., Feng, P., Xiu, H.-J., Li, J.-Y., Yang, X., Ma, F.-Y., Li, X., Zhang, X.-F., Kozliak, E., and Ji, Y. (2019). "Morphological changes of lignin during separation of wheat straw components by the hydrothermal-ethanol method," *Bioresource Technology* 294, article no. 122157. DOI: 10.1016/j.biortech.2019.122157
- Li, Y.-L., Wu, M., Wang, B., Wu, Y.-Y., Ma, M.-G., and Zhang, X.-M. (2016). "Synthesis of magnetic lignin-based hollow microspheres: A highly adsorptive and reusable adsorbent derived from renewable resources," *ACS Sustainable Chemistry & Engineering* 4(10), 5523-5532. DOI: 10.1021/acssuschemeng.6b01244
- Lievonen, M., Valle-Delgado, J. J., Mattinen, M.-L., Hult, E.-L., Lintinen, K., Kostiainen, M. A., Paananen, A., Szilvay, G. R., Setälä, H., and Österberg, M. (2016). "A simple process for lignin nanoparticle preparation," *Green Chemistry* 18(5), 1416-1422. DOI: 10.1039/c5gc01436k
- Luo, T., Wang, C., Ji, X.-X., Yang, G.-H., Chen, J.-H., Yoo, C. G., Janaswamy, S., and Lyu, G.-J. (2021). "Innovative production of lignin nanoparticles using deep eutectic solvents for multifunctional nanocomposites," *International Journal of Biological Macromolecules* 183, 781-789. DOI: 10.1016/j.ijbiomac.2021.05.005
- Lv, H.-S., Zhang, M., Geng, Z., Ren, M., and Sun, Y. (2013). "Influence of supercritical CO₂ pretreatment of corn stover with ethanol - Water as co-solvent on lignin degradation," *Chemical Engineering & Technology* 36(11), 1899-1906. DOI: 10.1002/cat.2013000183
- Monteiro, V. A. C., da Silva, K. T., da Silva, L. R. R., Mattos, A. L. A., de Freitas, R. M., Mazzetto, S. E., Lomonaco, D., and Avelino, F. (2021). "Selective acid precipitation of Kraft lignin: A tool for tailored biobased additives for enhancing PVOH films

- properties for packaging applications,” *Reactive and Functional Polymers* 166, article no. 104980. DOI: 10.1016/j.reactfunctpolym.2021.104980
- Nair, S. S., Sharma, S., Pu, Y.-Q., Sun, Q.-N., Pan, S.-B., Zhu, J. Y., Deng, Y.-L., and Ragauskus, A. J. (2014). “High shear homogenization of lignin to nanolignin and thermal stability of nanolignin-polyvinyl alcohol blends,” *ChemSusChem* 7(12), 3513-3520. DOI: 10.1002/cssc.201402314
- Ni, S.-Z., Bian, H.-Y., Zhang, Y.-C., Fu, Y.-J., Liu, W.-X., Qin, M.-H., and Xiao, H.-N. (2022). “Starch-based composite films with enhanced hydrophobicity, thermal stability, and UV-shielding efficacy induced by lignin nanoparticles,” *Biomacromolecules* 23(3), 829-838. DOI: 10.1021/acs.biomac.1c01288
- Posoknistakul, P., Tangkrakul, C., Chaosuanphae, P., Deepenthom, S., Techasawong, W., Phonphirunrot, N., Bairak, S., Sakdaronnarong, C., and Laosiripojana, N. (2020). “Fabrication and characterization of lignin particles and their ultraviolet protection ability in PVOH composite film,” *ACS Omega* 5(33), 20976-20982. DOI: 10.1021/acsomega.0c02443
- Stamenic, M., Zizovic, I., Eggers, R., Jaeger, P., Heinrich, H., Roj, E., Ivanovic, J., and Skala, D. (2010). “Swelling of plant material in supercritical carbon dioxide,” *The Journal of Supercritical Fluids* 52(1), 125-133. DOI: 10.1016/j.supflu.2009.12.004
- Wang, C.-Z., Li, H.-Y., Li, M.-F., Bian, J., and Sun, R.-C. (2017). “Revealing the structure and distribution changes of *Eucalyptus* lignin during the hydrothermal and alkaline pretreatments,” *Scientific Reports* 7(1), 1-10. DOI: 10.1038/s41598-017-00711-w
- Yang, M.-Y., Zhang, X., Guan, S.-Y., Dou, Y., and Gao, X.-F. (2020). “Preparation of lignin containing cellulose nanofibers and its application in PVOH nanocomposite films,” *International Journal of Biological Macromolecules* 158, 1259-1267. DOI: 10.1016/j.ijbiomac.2020.05.044
- Yang, W., Owczarek, J. S., Fortunati, E., Kozanecki, M., Massaglia, A., Balestra, G. M., Kenny, J. M., Torre, L., and Puglia, D. (2016). “Antioxidant and antibacterial lignin nanoparticles in polyvinyl alcohol/chitosan films for active packaging,” *Industrial Crops and Products* 94, 800-811. DOI: 10.1016/j.indcrop.2016.09.061
- Yiamsawas, D., Baier, G., Thines, E., Landfester, K., and Wurm, F. R. (2014). “Biodegradable lignin nanocontainers,” *RSC Advances* 4(23) 11661-11663. DOI: 10.1039/c3ra47971d
- Zhang, H.-D., and Wu, S.-B. (2015). “Pretreatment of eucalyptus using subcritical CO₂ for sugar production,” *Journal of Chemical Technology & Biotechnology* 90(9), 1640-1645. DOI: 10.1002/jctb.4470
- Zhang, H.-N., Zhao, J., Xu, D.-L., and Ren, H. (2018). “Structural features comparison of milled wood lignin and lignocresol by 2D-NMR spectra,” *Journal of Cellulose Science and Technology* 26(04), 9-18.
- Zhang, X., Yong, M.-K., Yan, Q.-P., and Cheng, G. (2019). “Controlled preparation of corncob lignin nanoparticles and their size-dependent antioxidant properties: Toward high value utilization of lignin,” *ACS Sustainable Chemistry & Engineering* 7(20), 17166-17174. DOI: 10.1021/acssuschemeng.9b03535
- Zhang, X., Liu, W.-F., Liu, W.-Q., and Qiu, X.-Q. (2020). “High performance PVOH/lignin nanocomposite films with excellent water vapor barrier and UV-shielding properties,” *International Journal of Biological Macromolecules* 142, 551-558. DOI: 10.1016/j.ijbiomac.2019.09.129

Zhao, G.-F., Ni, H.-Y., Ren, S.-X., and Fang, G.-Z. (2018). "Correlation between solubility parameters and properties of alkali lignin/PVOH composites," *Polymers* 10(3), 290. DOI: 10.3390/polym10030290

Article submitted: September 6, 2022; Peer review completed: October 1, 2022; Revised version received and accepted: October 9, 2022; Published: October 14, 2022.
DOI: 10.15376/biores.17.4.6598-6616